

$\phi \rightarrow 3\pi$ decay with Khuri-Treiman equations

A.G. Lorenzo, M. Albaladejo, S. González-Solís, A. Szczepaniak

Instituto de Física Corpuscular

QNP 2024 - Barcelona



VNIVERSITAT
ID VALÈNCIA

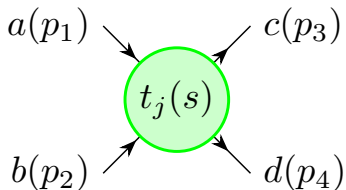


CSIC



GENERALITAT
VALENCIANA

Necessity of Khuri-Treiman Equations



Only Right-Hand Cut:

- Bethe-Salpeter equation.
- Dispersive Relations.
- K-matrix formalism.

What we have...

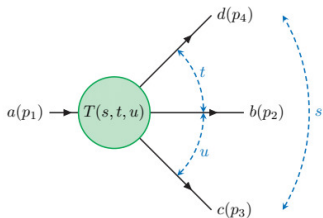
- Partial wave expansion **in the s-channel**:

$$T(s, t, u) = \sum_{j=0}^{\infty} (2j + 1) P_j(z_s) t_j(s)$$

- Infinite number of partial waves \Rightarrow requires truncation.
- Have both discontinuities: **RHC** and **LHC**.
- It can only reproduce poles in the s-channel.
- Crossing symmetry and unitarity are not fully recovered.

What we want...

- Handling of final states interactions (**FSI**).
- Simplified approach to discontinuities (with focus on **RHC**).
- Restoration of crossing symmetry.
- Analytic properties of amplitudes.
- Recover the unitarity of each channel (**t,u-channels**).
- Description of resonances.
- Versatility: be applied to a variety of processes, including three-body decays.



Limitations:

- High-energy limitations.
- Numerical challenges.
- Model dependence.

What we do...

Khuri-Treiman Equations: conceived to achieve the two-body unitarity in the three channels. — [N. Khuri, S. Treiman, *Phys. Rev.* 119 , 1115 (1960)]

- Consider three (s,t,u-channels) truncated **isobar** expansions:

$$T(s, t, u) = \sum_{j=0}^{\infty} (2j+1) P_j(z_s) t_j(s) \\ = \sum_{j=0}^{j_s} (2j+1) P_j(z_s) f_j^{(s)}(s) + \sum_{j=0}^{j_t} (2j+1) P_j(z_t) f_j^{(t)}(t) + \sum_{j=0}^{j_u} (2j+1) P_j(z_u) f_j^{(u)}(u)$$

- s-channel singularities appear in $f_j^{(s)}(s)$.
- \Rightarrow t,u-channel singularities are recovered in $f_j^{(t)}(t)$ and $f_j^{(u)}(u)$.
- LHC** of $t_j(s)$ are given by the **RHC** of the crossed channel isobars:

$$t_j(s) = \frac{1}{2} \int dz P_j(z) T(s, t', u') = f_j^{(s)}(s) + \underbrace{\frac{1}{2} \int dz Q_{j,j'}(s, t') f_{j'}^{(t)}(t')}_{\widehat{f}_j^{(s)}(s)}$$

Our Decay ...

$$\phi(p_1) \rightarrow \pi^+(p_2) \pi^0(p_3) \pi^-(p_4)$$

... is the combination of these three channels:

- **s-channel:** $\phi(p_1)\pi^0(-p_3) \rightarrow \pi^+(p_2)\pi^-(p_4)$
- **t-channel:** $\phi(p_1)\pi^(-p_2) \rightarrow \pi^0(p_3)\pi^-(p_4)$
- **u-channel:** $\phi(p_1)\pi^+(-p_4) \rightarrow \pi^+(p_2)\pi^0(p_3)$

- Initial state $\phi(1^{--}) \Rightarrow$ Final state $J = 1, 3, 5...$
- Three helicity states $\lambda = +1, 0, -1$.

- Parity: $\mathcal{H}_0 = 0$ y $\mathcal{H}_+ = \mathcal{H}_-$.
- Helicity amplitude:

$$\mathcal{M}_+ = \frac{\sqrt{\phi(s, t, u)}}{2} F(s, t, u)$$

Disclaimer!

The \mathcal{H}_λ are not Lorentz invariant but...

$$|\mathcal{M}|^2 = \frac{1}{3} \sum_{\lambda=+1,0,-1} |\mathcal{H}_\lambda|^2$$

...is indeed.

- Kibble function:

$$\phi(s, t, u) = 4sp^2(s)q^2(s) \sin^2 \theta_s$$

- Decay width:

$$\frac{d^2\Gamma}{dsdt}(s, t) \sim \phi(s, t, u) |F(s, t, u)|^2$$

Kibble function

$\phi(s, t, u)$ determine the possible accessible states of the phase space:

- $\phi(s, t, u) > 0 \Rightarrow$ **Allowed**
- $\phi(s, t, u) < 0 \Rightarrow$ **Forbidden**

Function $F(s, t, u)$:

All the dynamics of the process is contained within this Lorentz invariant amplitude!!!

Why revisit $\phi \rightarrow 3\pi$?

- Studies of the same decay have been conducted before, but not like in this work. — [F. Niecknig, B. Kubis y S. P. Schneider, *Eur. Física. JC 72 (2012) 2014*]
- We can compare it to the decay $\omega \rightarrow 3\pi$.
- Recent measurements of the TFF (2015) by KLOE.

Solving Khuri-Treiman Equations

- 1 Start with partial wave decomposition:

$$F(s, t, u) = \sum_{j \text{ odd}}^{\infty} (p(s)q(s))^{j-1} P'_j(\cos \theta_s) f_j(s) = f_1(s) + \dots$$

- 2 Do the truncated isobar expansion:

Consider only $j = 1$ (ρ) isobar

$$F(s, t, u) = F^{(s)}(s) + F^{(t)}(t) + F^{(u)}(u)$$

Isospin Limit:

$$= F(s) + F(t) + F(u)$$

- 3 Make the PW projection of the KT decomposition:

- Isobar: $f(s) = \mathbf{F}(s) + \hat{F}(s)$
- Inhomogeneity: $\hat{\mathbf{F}}(\mathbf{s}) = \frac{3}{2} \int_{-1}^1 dz_s (1 - z_s^2) F(t(s, z_s))$

- 4 Impose the DR relation at discontinuity to preserve unitarity:

$$\Delta F(s) = F(s + i\epsilon) - F(s - i\epsilon) = 2i \underbrace{\rho(s) (t_l^{2 \rightarrow 2}(s))^*}_{\sin \delta_l(s) e^{-i\delta_l(s)\theta(s-4m^2)}} (F(s) + \hat{F}(s))$$

5 Subtract ... or not:

Unsubtracted DR

$$F(s) = \frac{1}{2\pi i} \int_{4m^2}^{\infty} ds' \frac{\Delta F(s')}{s' - s}$$

- \mathbb{C}^1 space: $F(s) = aF_0(s)$
- $F_0(s) = \Omega(s) \left[1 + \frac{s}{\pi} \int_{4m^2}^{\infty} ds' \frac{\sin \delta(s') \hat{F}_0(s')}{s' |\Omega(s')| (s' - s)} \right]$

Advantages of subtraction:

- Enhances accuracy with data.
- Manage kinematic singularities and inelastic contributions.

Once-subtracted DR

$$F(s) = F(0) + \frac{s}{2\pi i} \int_{4m^2}^{\infty} ds' \frac{\Delta F(s')}{s'(s' - s)}$$

- \mathbb{C}^2 space:
 $F(s) = a [F_a(s) + bF_b(s)]$
- $F_a(s) = \Omega(s) \left[1 + \frac{s^2}{\pi} \int_{4m^2}^{\infty} ds' \frac{\sin \delta(s') \hat{F}_a(s')}{s'^2 |\Omega(s')| (s' - s)} \right]$
- $F_b(s) = \Omega(s) \left[s + \frac{s^2}{\pi} \int_{4m^2}^{\infty} ds' \frac{\sin \delta(s') \hat{F}_b(s')}{s'^2 |\Omega(s')| (s' - s)} \right]$

Disadvantages of subtraction:

- More parameters \Rightarrow Additional uncertainties.

In principle, the two solutions are different, but there must be some value of b for which they coincide...

Unsubtracted Sol.



Once-subtracted Sol.

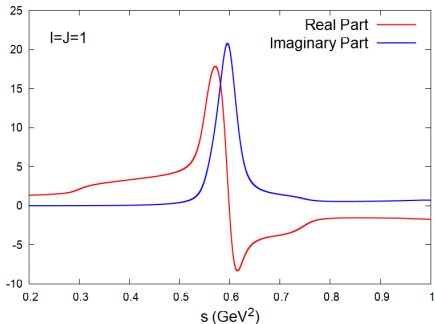
...which we call:

Sum Rule:

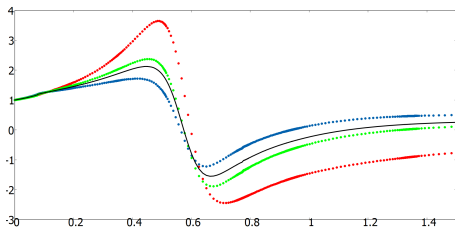
$$b_{\text{sum}} \equiv \frac{1}{\pi} \int_{4m^2}^{\infty} ds' \frac{\sin \delta(s') \hat{F}(s')}{s'^2 |\Omega(s')|}$$

Omnès Function:

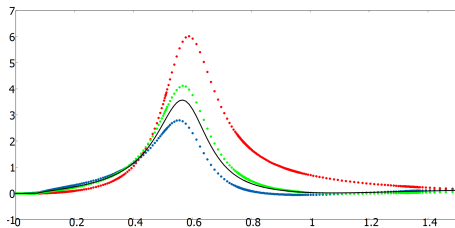
$$\Omega(s) = e^{\frac{s}{\pi} \int_{4m^2}^{\infty} ds' \frac{\delta(s')}{s'(s'-s)}}$$



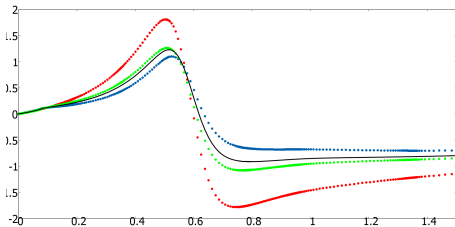
6 Iterate!



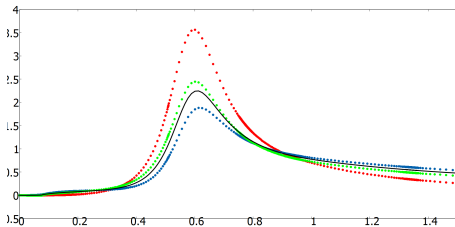
$\Re \{F_a(s)\}$ vs $s(\text{GeV}^2)$



$\Im \{F_a(s)\}$ vs $s(\text{GeV}^2)$



$\Re \{F_b(s)\}$ vs $s(\text{GeV}^2)$



$\Im \{F_b(s)\}$ vs $s(\text{GeV}^2)$

$\phi \rightarrow \gamma^* \pi^0$ Transition Form Factor

- The decays $\phi(\rightarrow \gamma^* \pi^0) \rightarrow \pi^0 l^+ l^-$ and $\phi \rightarrow \gamma \pi^0$ are governed by the **TFF** $f_{\phi\pi^0}(s)$:

- Amplitude: $\mathcal{M} = f_{\phi\pi^0}(s) \epsilon_{\nu\mu\alpha\beta} \epsilon^\mu(p_\phi, \lambda) p^\nu q^\alpha \frac{ie^2}{s} \bar{u}(p_-) \gamma^\beta v(p_+)$
- Decay width: $\Gamma = |f_{\phi\pi^0}(0)|^2 \frac{e^2(M_\phi^2 - m_{\pi^0}^2)^3}{96\pi M_\phi^3}$

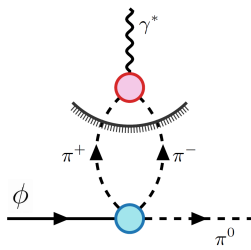
- Dispersive representation:

$$\Delta f_{\phi\pi^0}(s) = i \frac{p^3(s)}{6\pi\sqrt{s}} F_\pi^{V^*}(s) f_1(s) \theta(s - 4m^2)$$

- Due to the low energy of the $\phi\pi^0$ system, we can take $F_\pi^{V^*}(s) \approx \Omega(s)$.

Once-subtracted DR:

$$f_{\phi\pi^0}(s) = |f_{\phi\pi^0}(0)| e^{i\theta_{\phi\pi^0}(0)} + \frac{s}{12\pi^2} \int_{4m^2}^{\infty} ds' \frac{1}{\sqrt{(s')^3}} \frac{p^3(s') \Omega(s') f_1(s')}{(s' - s)}$$



From $\phi \rightarrow 3\pi$ amplitude $F(s, t, u)$

- A real global normalization $|a|$.
- A complex parameter $b = b_r + ib_i$ from the once-subtracted solution.

From $\phi \rightarrow \gamma^*\pi^0$ TFF $f_{\phi\pi^0}(s)$

- A real normalization of the TFF $|f_{\phi\pi^0}(0)|$.
- A relative phase $\theta_{\phi\pi^0}$ between $f_{\phi\pi^0}(0)$ and $f_{3\pi}(0)$.

ρ^0 and ω mixing

Due to the fact that they share the same quantum numbers 1^{--} , they can mix.

- A complex coupling constant A on the s-channel:

$$F(s) \rightarrow F(s) + A \frac{M_\omega^2}{M_\omega^2 - \sqrt{s}\Gamma_\omega i - s}$$

Global Parameters

- A real parameter N that serves as an adjustable parameter for the total number of events.

Global Input

The phase-shift $\delta_i(s)$ parametrization of the $\pi\pi$ P-wave. (We take the 4 of them to compare).

— *Madrid Group Phys.Rev.D69:114001,2004 and Phys.Rev.D83:094011*

To fit $\phi \rightarrow 3\pi$ amplitude $F(s, t, u)$

Dalitz Plot divided in bins.

$$(X_i, Y_i) \leftrightarrow (s_i, t_i)$$

— *KLOE collaboration*

To fit $\phi \rightarrow \gamma^*\pi^0$ TFF $f_{\phi\pi^0}(s)$

Measurement of the normalized TFF.

$$\left| \frac{f_{\phi\pi^0}(s)}{f_{\phi\pi^0}(0)} \right|^2$$

— *KLOE collaboration*

Particle Data Group

$$\Gamma_\phi, \mathcal{B}(\phi \rightarrow 3\pi), \mathcal{B}(\phi \rightarrow \gamma\pi^0), M_\omega, \Gamma_\omega$$

General Chi-Square χ^2

$$\chi^2 \equiv \chi_{DP}^2 + \chi_{\Gamma_{3\pi}}^2 + \chi_{TF}^2 + \chi_{\Gamma_{\pi^0\gamma}}^2$$

- $\chi_{DP}^2 = \sum_i \left(\frac{N_{ev,i}^{exp} - N_{ev,i}^{th}}{\sigma_{N_{ev,i}^{exp}}} \right)^2$ with

$$N_{ev,i}^{exp} = \frac{N}{(2\pi)^3 384 M_\phi^3} \frac{1}{2\Delta s \Delta t} \int_{s_i - \Delta s}^{s_i + \Delta s} \int_{t_i - \frac{(s-s_i) - \Delta t}{2}}^{t_i - \frac{(s-s_i) + \Delta t}{2}} \phi(s, t) |F(s, t)|^2 dt ds$$

- $\chi_{\Gamma_{3\pi}}^2 = \left(\frac{\Gamma_{3\pi}^{exp} - \Gamma_{3\pi}^{th}}{\sigma_{\Gamma_{3\pi}^{exp}}} \right)^2$ with $\Gamma_{3\pi}^{th} = \frac{1}{(2\pi^3) 384 M_\phi^3} \int_{4m^2}^{\infty} \int_{t_-}^{t_+} \phi |F(s, t)|^2 dt ds$

- $\chi_{TF}^2 = \sum_i \left(\frac{\left| \frac{f_{\phi\pi^0}(s_i)}{f_{\phi\pi^0}(0)} \right|_{exp}^2 - \left| \frac{f_{\phi\pi^0}(s_i)}{f_{\phi\pi^0}(0)} \right|_{exp}^2}{\sigma_i^{TF}} \right)^2$ with

$$\left| \frac{f_{\phi\pi^0}(s_i)}{f_{\phi\pi^0}(0)} \right|_{th}^2 = \frac{1}{4\sqrt{s_i}\Delta\sqrt{s_i}} \int_{(\sqrt{s_i} - \Delta\sqrt{s_i})^2}^{(\sqrt{s_i} + \Delta\sqrt{s_i})^2} \left| \frac{f_{\phi\pi^0}(s)}{f_{\phi\pi^0}(0)} \right|^2 ds$$

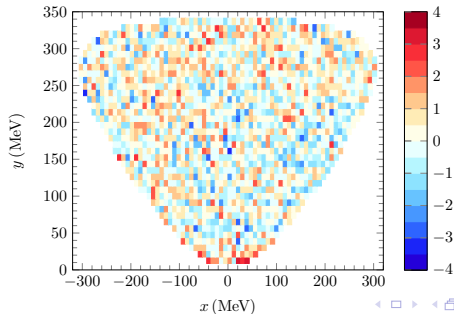
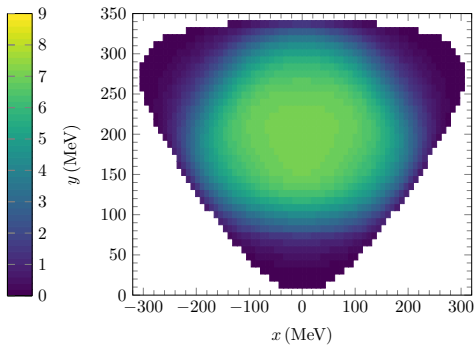
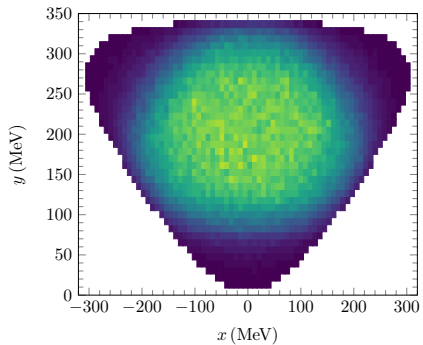
- $\chi_{\Gamma_{\phi\pi^0}}^2 = \left(\frac{\Gamma_{\phi\pi^0}^{exp} - \Gamma_{\phi\pi^0}^{th}}{\sigma_{\Gamma_{\phi\pi^0}^{exp}}} \right)^2$

		δ_1	δ_2	δ_3	δ_4
$ a $	$[\text{GeV}^{-3}]$	15.60(23)	15.16(22)	15.23(22)	15.07(22)
$\Re(b)$	$[\text{GeV}^{-2}]$	0.690(19)	0.810(17)	0.788(17)	0.819(16)
$\Im(b)$	$[\text{GeV}^{-2}]$	0.312(30)	0.570(40)	0.545(38)	0.594(40)
$\Re(A)$	$[\text{GeV}^{-3}]$	0.1251(98)	0.1208(97)	0.1208(97)	0.1212(97)
$\Im(A)$	$[\text{GeV}^{-3}]$	0.025(12)	0.053(12)	0.050(12)	0.056(12)
$ f_{\phi\pi^0}(0) $	$[\text{GeV}^{-1}]$	0.1351(26)	0.1351(26)	0.1351(26)	0.1351(26)
$\theta_{\phi\pi^0}(0)$		0.40(17)	0.50(17)	0.48(17)	0.50(17)
N_{ev}	$[10^6]$	6.60(10)	6.60(10)	6.60(10)	6.60(10)
χ^2/d		1.012	1.029	1.026	1.0309

Fit utilities

- We make use of the library Minuit2 of C++, with Migrad, Minos and Covariance as subroutines.
- Montecarlo Resampling (M.C.) of 10^5 for each $\delta_i(s)$.
- Total number of points (with $\phi(s_i, t_i) > 0$ criteria):

$$N = N_{DP} + N_{\Gamma_{3\pi}} + N_{TF} + N_{\Gamma_{\pi^0\gamma}} = 1860 + 1 + 15 + 1 = 1877$$

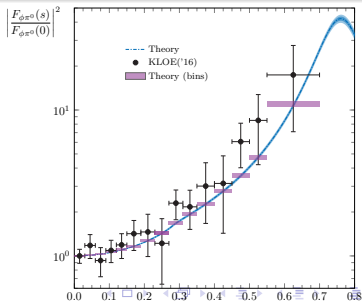
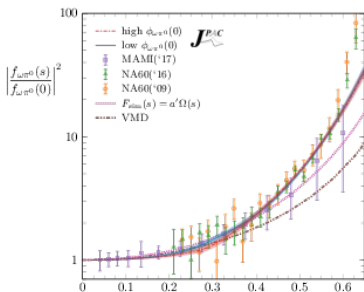


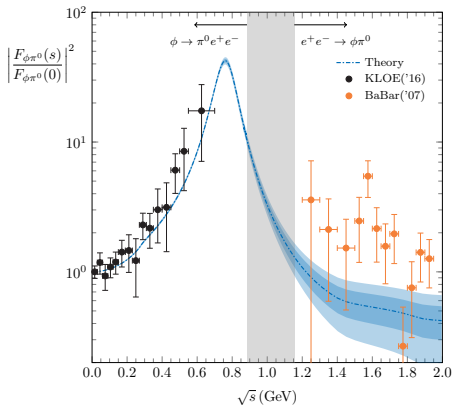
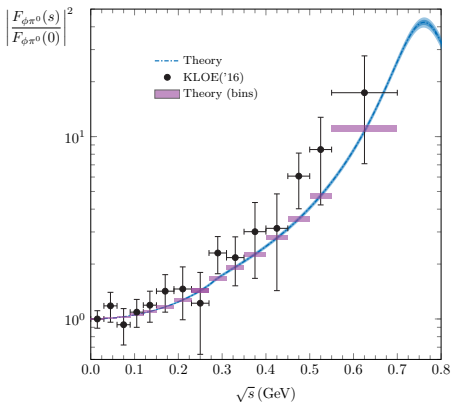
	δ_1	δ_2	δ_3	δ_4
$\Re(b_{\text{sum}})$	0.61279	0.65841	0.62613	0.62081
$\Im(b_{\text{sum}})$	0.50581	0.52535	0.52288	0.52413
$\Re(b)$	0.690(19)	0.810(17)	0.788(17)	0.819(16)
$\Im(b)$	0.312(30)	0.570(40)	0.545(38)	0.594(40)

Sum rule for $\omega \rightarrow 3\pi$

$$b_{\text{sum}} = 0.54382 + 0.08219i \quad b_{\text{fit}} = -0.341(40) + 2.62(79)i$$

— JPAC collaboration *Eur. Phys. J. C* (2020) 80:1107





Disclaimer!

- We haven't fitted the data from the BaBar experiment.
- KT formalism is not prepared for high energies.
- We can still observe a good trend in them!!

Conclusions

- Difference between the results of the fit and the same values computed through the sum rule \Rightarrow Justify the need of the extra subtraction.
- The values of the transition form factor given by the Khuri-Treiman approach with the additional subtraction used for our process are in very good agreement with the experimental data.
- For high energies, there is a good trend of what happens in the dispersive region.
- A different trend compared to the ω decay, there must be physics behind that process that has not been taken into account.